Hollow-core optical fiber with eight-pointed star cladding structure for low-loss transmission in telecom bands

Mustafa ORDU[*]

UNAM–National Nanotechnology Research Center and Institute of Materials Science and Nanotechnology
Bilkent University, Ankara, Turkey

Abstract: In this study, a novel negative curvature hollow-core fiber is proposed for low-loss transmission in the near-infrared region. We numerically investigate the effect of the cladding structure, which is formed of concentrically interlaced squares, to the confinement losses using the finite element modelling. The design has eight cladding tubes with nested elements placed to the outer edge of the tubes. The confinement losses of the interlaced square core fiber is calculated as low as 0.12 dB/km in the range of 1.3 to 1.65 μm. The loss profile of the noncircular core design is comparable with the circular cores, and have improved transmission performance at 1.55 μm. The proposed design can have numerous application areas such as data transmission, nonlinear optics and biochemical sensing.

Key words: Hollow-core fibers, negative curvature fibers, numerical modeling, fiber design

1. Introduction

Hollow-core photonic crystal fibers (HC-PCF, shortened as HCF in this work) were first proposed at the edge of the new millennia and rapidly attracted attention due to their extraordinary optical guidance properties [1, 2]. HCFs are capable of guiding light through the hollow-core by means of the microstructured cladding that is composed of holes and glass struts. High damage threshold, low transmission losses in the visible and near-infrared (near-IR) regions, gas-light interaction in a confined environment and reduced latency are some of their advantages that have lead for various applications such as low-loss light guidance, ultrafast pulse propagation and biochemical sensing [3–5]. Moreover, HCFs are free of the Fresnel reflection that is one of the major sources of losses in the solid core fibers. Today, the optical transmission in the telecom bands (1260–1625 nm) heavily depends on the solid core silica optical fibers that are limited by the Rayleigh scattering of the silica [6]. HCFs can surpass this limit by guiding the light through the air or other gases that has much lower Rayleigh limit than glasses. A new group of HCF, negative curvature hollow-core fibers (NC-HCFs) have recently achieved to have lower losses than the silica in the visible range and this promising result makes the NC-HCF one of the strongest candidates to break the Rayleigh limit in the near-IR region as well [7, 8].

Several studies have proposed novel designs of low-loss NC-HCF for the near-IR with various cladding elements such as Kagome [9], circular tubes [10, 11], nested tubes [12], conjoined tubes [13], elliptical tubes [14, 15], lotus-shaped tubes [16], extended tubes [17], "ice cream cone" tubes [18], positively-negatively curved bars within tubes [19] and hybrid Kagome-tubular [20]. Also, a remarkable method of designing NC-HCF by using a reinforcement learning based method was also presented [21]. The numerical studies on the nested-

---

[*]Correspondence: ordu@unam.bilkent.edu.tr

tubular NCF (also called as nested antiresonant nodeless fiber; NANF) predict low-loss transmission in the telecom band i.e. 0.2 dB/km [12]. The experimental demonstration achieved a minimum of 0.28 dB/km transmission loss between 1.51 and 1.6 μm [22]. The difference between the numerical and experimental studies mainly originates from the fabrication-related imperfections. The further design improvement over the nested-tubular design can overcome this problem to break the low-loss record of the solid core silica optical fibers in the telecom bands [23].

This work proposes a novel HCF design with interlaced squares cladding structure for low-loss transmission in the near-IR region. The primary design parameters of the proposed structure were determined via computer simulations at the target wavelength of 1.55 μm. A 0.12 dB/km confinement loss was achieved at 1.55 μm within the low-loss region (0.2 dB/km) between 1.3 to 1.65 μm. The proposed design will be an important step for the next generation low-loss telecom fibers.

2. Numerical methodology and fiber design

The guidance mechanism of the NC-HCFs is based on inhibited coupling, and light is confined in the hollow-core by the low spatial overlap of core and cladding modes and strong phase mismatch between these modes [24]. The transmission losses of NC-HCFs are mainly originated from three sources: surface scattering loss (SSL), ultraviolet (UV) absorption and confinement loss (CL). SSL and UV absorption are the dominant loss mechanism at the UV and visible light regions whereas in the near-IR region, the losses are mainly originated due to the CL. To begin the design of a low-loss HCF, there are several important criteria to consider. Firstly, the transmission window of an HCF is divided by high loss resonant wavelengths that are calculated by:

$$\lambda_{\mathrm{m}} \approx \frac{2t\sqrt{(n^2_{\mathrm{glass}} - n^2_{\mathrm{air}})}}{m} \tag{1}$$

Here, t is the strut thickness, n_{glass} is the refractive index of glass, n_{air} is the refractive index of air, and m is an integer number as m=1,2,3... etc. n_{glass} is selected as the refractive index of fused silica that is used to design the EPS-NCF. For each λ_{m}, the resonance occurs due to the strong anticrossing between the air and glass modes in the HCFs. Therefore, the selection of the strut thickness is important to achieve low-loss operation in the targeted telecom bands: S-band (1460–1530 nm), C-band (1530–1565 nm) and L-band (1565–1625 nm). The design wavelength is selected as 1.55 μm in the C-band for the initial calculation. Secondly, nodes, connection points of the cladding elements, negatively affects the transmission by acting as a strong anticrossing points for air and glass modes. Thus, isolation of the nodes from the light is crucial to decrease the losses. The transmission losses becomes high when the cladding elements around the hollow-core are in flat or positively curved shapes i.e. convex strut, due to the increased interaction between the light and the nodes. The light confinement can be improved by forming negatively curved elements i.e. concave strut, around the hollow-core. The effect of the curvature to the optical transmission was systematically investigated with a set of Kagome HCFs by varying the negative curvature around the hollow-core [25]. Adjusting the pressurization during the fiber drawing leads to circular or even elliptical elements over the first cladding layer of the Kagome HCF. This process considerably lowered the transmission losses and shows the important effect of the curvature to the light. Here, we selected independent tubular cladding elements that are the simplified design of the Kagome HCF and provide a robust structure to create the same lowering effect of the negative curvature to the confinement loss [10, 26]. Thirdly, nesting additional elements within the cladding tubes was found to be an important design improvement to prevent light coupling to the outer silica cladding [12]. This effect was

also verified with elliptical nested elements [15]. Lastly, the leakage of the light between the cladding tubes is another source of loss and redesigning the parts between the tubes can even lead to an improvement over the light confinement in the hollow-core. Combining all the design criteria, we proposed a hollow-core negative curvature fiber with eight-pointed star cladding (EPS-NCF).

Figure 1a shows the cross-sectional image of the EPS-NCF with the primary design parameters: $\varnothing_{core}$ is the core diameter, $\varnothing_{tube}$ is the tube diameter, $\varnothing_{nest}$ is the nested tube diameter, and t is the strut thickness. The fiber cladding is formed by concentrically interlacing two identical squares one of which is rotated by an angle of 45 degrees leading to an eight-pointed star shape. Cladding tubes are placed at each corner of the eight-pointed star with nested elements placed inside of them. Selected thickness of the silica struts is 0.44 μm for minimum losses between 1.3 to 1.6 μm that covers the most of S, C and L telecom bands. Furthermore, the core diameter, that is the shortest distance between two oppositely located cladding tubes, is kept constant at 40 μm. Larger core diameters generally have lower transmission losses but in return the flexibility of the fiber decreases. Therefore an NCF with a 40-μm core diameter has $\sim$300 μm outer diameter that satisfies for both low-loss operation and good flexibility. It is worth mentioning that, a 300-μm outer diameter value includes the outer silica cladding that will support the microstructured inner part of the cladding.

COMSOL Multiphysics was used to design and simulate the fibers with a finite element methods (FEM) based electromagnetic field solver. In this work, the quarter of the original fiber geometry was used to improve the efficiency of the computational time by exploiting the symmetric fiber design. The mesh size is defined as $\lambda/5$ for the entire structure by maintaining minimum 5 elements at the narrow regions. The meshed quarter fiber is shown in Figure 1b. The densely meshed narrow regions of the cladding elements are easily distinguishable in the core region. The perfectly matched layer (PML) was optimized based on the previous studies, and a circular 10-µm thick PML was used around of the fiber [12, 27]. The simulation models were run to find the optimum design parameters at 1.55 μm. The final structure was compared with the circular core designs between 1.3 and 2.0 μm. Figure 1c shows the electric field of the quarter EPS-NCF with the fundamental mode at 1.55 μm. The sharp corners were slightly rounded to create a realistic model of a drawn fiber.
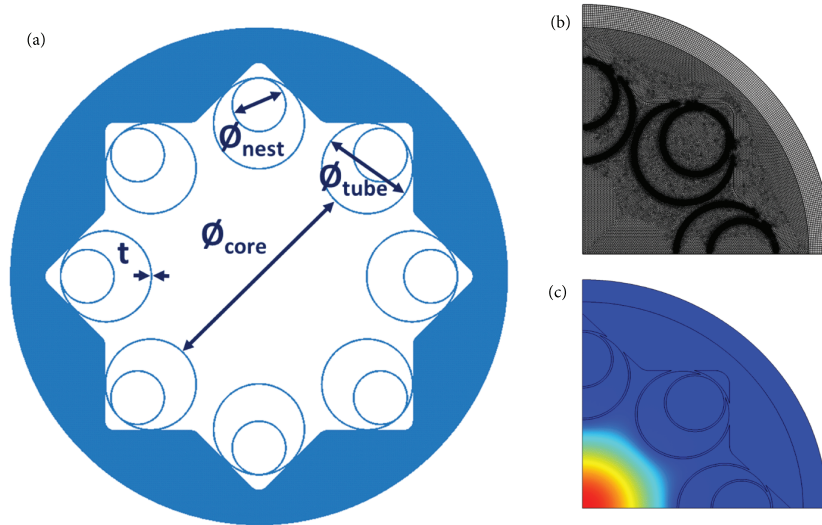

Figure 1. a) Schematic cross-sections of the EPS-NCF with the important design parameters: Core diameter, $\varnothing_{core}$, tube diameter, $\varnothing_{tube}$, nested tube diameter, $\varnothing_{nest}$, and strut thickness, t. b) Meshed quarter cross-section of the EPS-NCF and (c) electric field distribution at 1.55 μm.

3. Simulation results

Figure 2 shows the simulation results of EPS-NCF for three design parameters. The confinement losses of the EPS-NCF for different diameter of the cladding tubes at 1.55 μm are given in Figure 2a. Between the values of 18 to 25 μm, the lowest loss was achieved with a diameter of 22.6 μm. Moreover, the cladding tubes are in contact when the diameter is greater than 25 μm, resulting in a sharp increase of losses due to the formation of additional nodes. Also, small cladding tubes lead to high losses due to the coupling of the guided light to the silica cladding. The effect of the nested tube diameter to the confinement losses at 1.55 μm is shown in Figure 2b. The loss reaches to a minimum when the diameter of nested tubes is 15 μm. Increasing the number of nested tubes will further improve the transmission performance of the NC-HCFs but in return it will increase the fabrication complexities [12]. It is worth mentioning that, the nested tube diameter in Figure 2a is initially approximated as $0.50 \times \varnothing_{tube}$. After the multiple iterations between the simulations of cladding tubes and nested tubes, $\varnothing_{nest}$ was selected as $0.66 \times \varnothing_{tube}$ for the optimum performance.

After the selection of $\varnothing_{tube}$ and $\varnothing_{nest}$, an additional scan was performed for the strut thickness between 0.30 to 0.60 μm, as shown in Figure 2c. Here, the initially defined thickness of 0.44 μm gives the lowest confinement loss at the targeted wavelength of 1.55 μm. Thus, we kept the strut thickness as 0.44 μm to ensure the low-loss operation through the fiber.
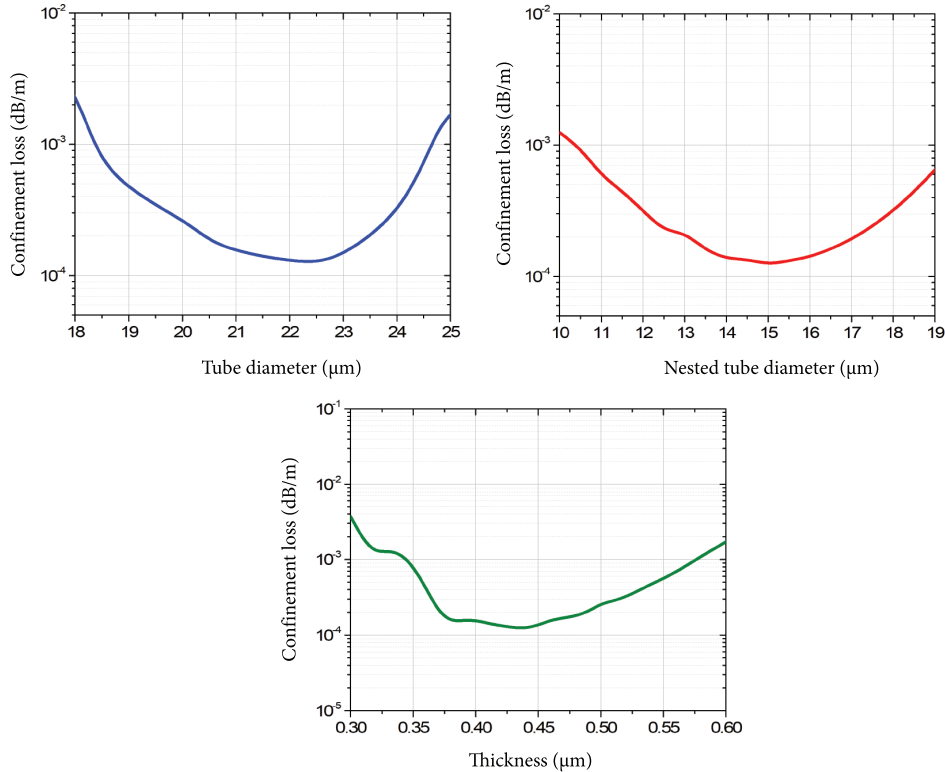

Figure 2. The simulation results of the major design parameters of EPS-NCF at 1.55 μm. (a) The confinement losses versus the diameter of cladding tubes. The loss becomes minimum with 18.6 μm cladding tubes. (b) The effect of the nested tube diameter to the confinement loss. The losses reach to minimum values around the diameter of 15 μm. (c) The strut thickness versus the confinement losses. The minimum losses is achieved with 0.44 μm.

The comparison of transmission losses for the EPS-NCF with the tubular and nested-tubular NCFs between 1.3 and 2.0 μm is shown in Figure 3. All three NCFs have the same core diameter (40 μm), strut

thickness (0.44 μm) and number of cladding tubes (8 cladding tubes with circular nested elements) for a reliable comparison. The EPS-NCF has approximately two order of magnitude lower transmission losses than tubular NCF and has a comparable light confinement with the nested-tubular NCF in the targeted range. Moreover, the calculated loss of EPS-NCF at 1.55 μm is 0.12 dB/km that is lower than the nested-tubular NCF ($\sim$0.2 dB/km).
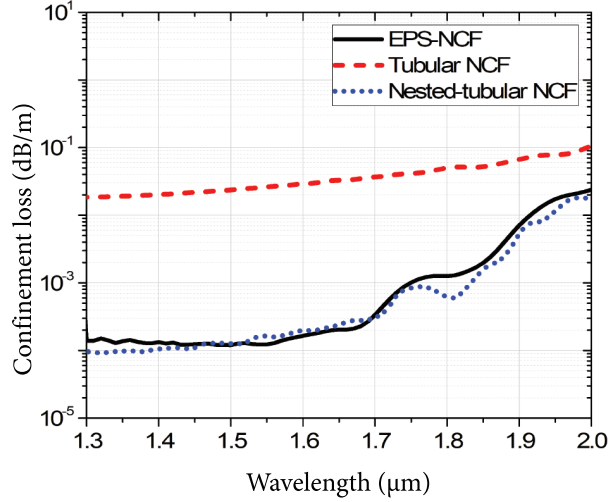

Figure 3. The comparison of the transmission losses of 8-NCF with the tubular and nested-tubular NCFs. The proposed design performs better at 1.55 μm.

In order to achieve a sub-0.1 dB/km loss in the telecom bands, a design upgrade over the EPS-NCF is necessary. This can be simple achieved by replacing the outer circular boundary of the silica cladding with a second interlaced square layer, as shown in Figure 4a. The new thickness of the outer silica cladding is 1 μm forming a eight-pointed star structure. The core diameter, strut thickness and the number of cladding elements remained same as 40 μm, 0.44 μm and 8, respectively. This design improvement dramatically decreases the confinement losses that reaches to 0.001 dB/km at the targeted region (Figure 4b). Although, the thin outer cladding causes additional resonant points, especially around 1.9 μm that are visible from the graph, the overall transmission performance of the new design is considerably better than the initial design as well as nested-tubular NCF . Moreover, the fabrication of the improved design would be substantially challenging since a thicker cladding is vital to support the fiber structure during the drawing and usage.

Lastly, we elaborate on the future fabrication and the preform design of EPS-NCF to achieve a successful demonstration of the fiber. The preform can be formed by stacking glass rods for the outer silica cladding and tubes for the inner cladding. The support tubes/rods are placed between the inner cladding tubes and hollow-core to prevent any collapse during the fiber draw. Precise control over the pressurization of the core and cladding during the fiber drawing might be necessary in order to achieve the desired structure. An additional vacuuming might be necessary at the outer cladding to collapse the gaps between the glass rods and to form a solid outer cladding.

Future efforts will focus on the characterization of EPS-NCF for bending losses and higher order mode suppression. Also new type of the EPS-NCF for shorter or longer wavelength operations will be investigated to expand the applicability of the HCFs. One important target region for the EPS-NCF would be the mid-IR
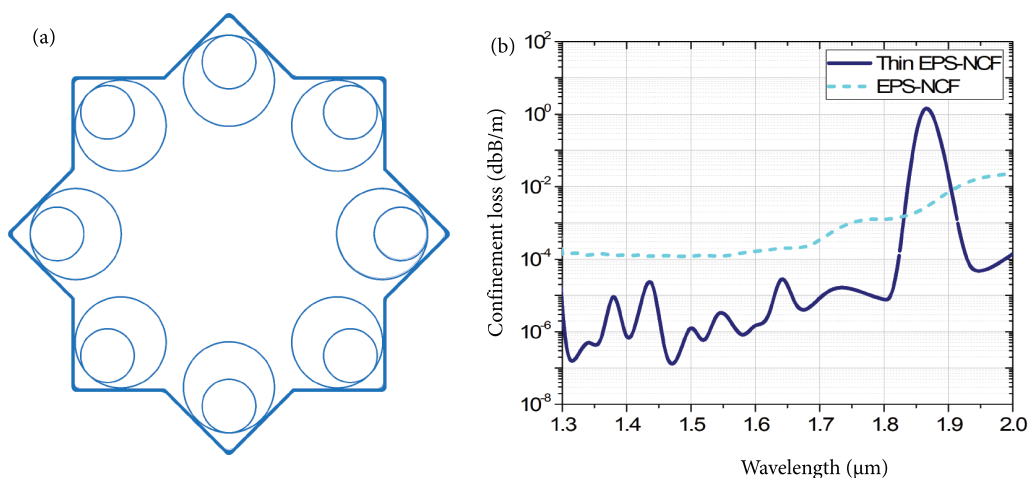
Figure 4. (a) A proposed improvement of the EPS-NCF with thin outer silica cladding. The decreases the confinement losses reaches to 0.001 dB/km in the telecom bands. (b) Simulated confinement losses of the improved EPS-NCF (Thin EPS-NCF) and regular EPS-NCF.

which still requires low-loss fibers for various applications such as remote laser delivery and chemical sensing [28, 29].

4. Conclusion

In summary, we proposed a novel NC-HCF design for low-loss operation in the telecom bands. The concentrically interlaced square design with nested cladding tubes has improved light confinement in the targeted spectrum and achieved 0.12 dB/km confinement loss at 1.55 μm that is lower than the tubular and nested-tubular NCFs. Comparing with the other designs, EPS-NCF can be fabricated similarly by elaborately stacking a combination of rods and tubes and controlling the core and cladding pressurization during the drawing processes. An ideal EPS-NCF design with thin outer glass cladding was also proposed for ultimate low-loss operation in the mid-IR albeit the limiting fabrication processes. Further improvement of the design can decrease the losses and widen the low-loss region as well as show bending sensitivity and higher order mode suppression. We believe that this proposed noncircular hollow-core structure is a promising alternative for near-IR light guidance, and it will facilitate the candidacy of NCFs to become the backbone of the future long haul optical fiber network.

Acknowledgment

References

[1] Cregan RF, Mangan BJ, Knight JC, Birks TA, Russell PS et. al. Single-mode photonic band gap guidance of light in air. Science 1999; 285 (5433):1537-1539.

[2] Debord B, Amrani F, Vincetti L, Gérôme F, Benabid F. Hollow-core fiber technology: the rising of "gas photonics". Fibers 2019; 7 (2): 16.

[3] Mangan BJ, Farr L, Langford A, Roberts PJ, Williams DP et al. Low loss (1.7 dB/km) hollow core photonic bandgap fiber. In: Optical Fiber Communication Conference; USA; 2004. p. 3.

[4] Cubillas AM, Unterkofler S, Euser TG, Etzold BJ, Jones AC et al. Photonic crystal fibres for chemical sensing and photochemistry. Chemical Society Reviews 2013; 42 (22): 8629-8648.

[5] Benabid F, Knight JC, Antonopoulos G, Russell PSJ. Stimulated Raman scattering in hydrogen-filled hollow-core photonic crystal fiber. Science. 2002; 298 (5592): 399-402.

[6] Ding W, Wang YY, Gao SF, Wang ML, Wang P. Recent progress in low-loss hollow-core anti-resonant fibers and their applications. IEEE Journal of Selected Topics in Quantum Electronics 2019; 26 (4): 1-2.

[7] Gao SF, Wang YY, Ding W, Hong YF, Wang P. Conquering the Rayleigh scattering limit of silica glass fiber at visible wavelengths with a hollow-core fiber approach. Laser & Photonics Reviews 2020; 14 (1): 1900241.

[8] Sakr H, Chen Y, Jasion GT, Bradley TD, Hayes JR et al. Hollow core optical fibres with comparable attenuation to silica fibres between 600 and 1100 nm. Nature Communications 2020; 11 (1).

[9] Wheeler NV, Bradley TD, Hayes JR, Gouveia MA, Liang S et al. Low-loss Kagome hollow-core fibers operating from the near-to the mid-IR. Optics Letters 2017; 42 (13): 2571-2574.

[10] Debord B, Amsanpally A, Chafer M, Baz A, Maurel M et al. Ultralow transmission loss in inhibited-coupling guiding hollow fibers. Optica 2017; 4 (2): 209-217.

[11] Hayes JR, Sandoghchi SR, Bradley TD, Liu Z, Slavík R et al. Antiresonant hollow core fiber with an octave spanning bandwidth for short haul data communications. Journal of Lightwave Technology 2017; 35 (3): 437-442.

[12] Poletti F. Nested antiresonant nodeless hollow core fiber. Optics Express 2014; 22 (20): 23807-23828.

[13] Gao SF, Wang YY, Ding W, Jiang DL, Gu S et al. Hollow-core conjoined-tube negative-curvature fibre with ultralow loss. Nature Communications 2018; 9 (1): 1-6.

[14] Habib MS, Bang O, Bache M. Low-loss single-mode hollow-core fiber with anisotropic anti-resonant elements. Optics Express 2016; 24 (8): 8429-8436.

[15] Meng FC, Liu BW, Li YF, Wang CY, Hu ML. Low loss hollow-core antiresonant fiber with nested elliptical cladding elements. IEEE Photonics Journal 2016; 9 (1): 1-11.

[16] Nawazuddin MB, Wheeler NV, Hayes JR, Sandoghchi SR, Bradley TD et al. Lotus-shaped negative curvature hollow core fiber with 10.5 dB/km at 1550 nm wavelength. Journal of Lightwave Technology 2017; 36 (5): 1213-1219.

[17] Ge A, Meng F, Li Y, Liu B, Hu M. Higher-order mode suppression in antiresonant nodeless hollow-core fibers. Micromachines 2019; 10 (2): 128.

[18] Belardi W, Knight JC. Effect of core boundary curvature on the confinement losses of hollow antiresonant fibers. Optics Express 2013; 21 (19):21912-21917.

[19] Hasan MI, Akhmediev N, Chang W. Positive and negative curvatures nested in an antiresonant hollow-core fiber. Optics Letters 2017; 42 (4): 703-706.

[20] Amrani F, Osório JH, Delahaye F, Giovanardi F, Vincetti L et al. Low-loss single-mode hybrid-lattice hollow-core photonic-crystal fibre. Light: Science & Applications 2021; 10 (1): 1-2.

[21] Hu X, Schülzgen A. Design of negative curvature hollow core fiber based on reinforcement learning. Journal of Lightwave Technology 2020; 38 (7):1959-1965.

[22] Jasion GT, Bradley TD, Harrington K, Sakr H, Chen Y et al. Hollow core NANF with 0.28 dB/km attenuation in the C and L bands. In: Optical Fiber Communication Conference; San Diego, CA, USA; 2020.

[23] Tamura Y, Sakuma H, Morita K, Suzuki M, Yamamoto Y et al. The first 0.14-dB/km loss optical fiber and its impact on submarine transmission. Journal of Lightwave Technology 2018; 36 (1): 44-49.

[24] Couny F, Benabid F, Roberts PJ, Light PS, Raymer MG. Generation and photonic guidance of multi-octave optical-frequency combs. Science 2007; 318 (5853): 1118-1121.

[25] Debord B, Alharbi M, Bradley T, Fourcade-Dutin C, Wang YY et al. Hypocycloid-shaped hollow-core photonic crystal fiber Part I: Arc curvature effect on confinement loss. Optics Express 2013; 21 (23): 28597-28608.

[26] Kolyadin AN, Kosolapov AF, Pryamikov AD, Biriukov AS, Plotnichenko VG et al. Light transmission in negative curvature hollow core fiber in extremely high material loss region. Optics Express 2013; 21 (8): 9514-9519.

[27] Wang Y, Hasan MI, Hassan MR, Chang W. Effect of the second ring of antiresonant tubes in negative-curvature fibers. Optics Express 2020; 28 (2):1168-1176.

[28] Tao G, Ebendorff-Heidepriem H, Stolyarov AM, Danto S, Badding JV et al. Infrared fibers. Advances in Optics and Photonics 2015; 7 (2): 379-458.

[29] Ordu M, Basu SN. Recent progress in germanium-core optical fibers for mid-infrared optics. Infrared Physics & Technology 2020; 111: 103507.